Peeling off an adhesive layer with spatially varying modulus

Animangsu Ghatak
Department of Chemical Engineering, Indian Institute of Technology, Kanpur, Uttar Pradesh 208016, India
(Received 3 November 2009; published 9 February 2010)

We analyze here displacement controlled peeling of a flexible adherent off a thin layer of elastic adhesive, the elastic modulus of which does not remain uniform but varies periodically along the direction of peeling. Calculation shows that with progressive peeling, the crack front does not propagate continuously at the interface but intermittently with crack arrests and subsequent initiations. The crack gets arrested close to the location of the minimum shear modulus of the layer and initiates again only at a sufficiently large peel off load. This effect is very similar to the peeling experiment off surface patterned and microchannel embedded adhesives which results in significant enhancement of fracture toughness of the interface over smooth adhesive layers. The fracture toughness of the interface increases with the increase in thickness of the layer and the amplitude of variation in modulus. Fracture toughness is calculated to be high also for the larger value of critical stress at the opening of the crack. With the wavelength of modulus variation, it varies nonmonotonically, maximizing at an intermediate value. These results define the criterion for designing adhesive layers with spatially modulated physical properties useful for variety of applications.

DOI: 10.1103/PhysRevE.81.021603 PACS number(s): 68.47.Pe, 68.35.Np, 68.35.Gy

I. INTRODUCTION

While adhesion in most practical situations involve a smooth layer of glue sandwiched between two rigid or flexible adherents, biological adhesives occurring at the feet of many living species, e.g., house lizards, geckos, tree frogs, and many insects, are far from homogeneous either in physical morphology or in material characteristics [1–3]. In fact, these adhesives are extensively patterned, their surfaces are hierarchically structured and they even have subsurface fluid filled vessels, e.g., air pockets [4], blood vessels [5,6], and glands [7–9], which too affect the mechanism of adhesion at the surface. Using this gamut of multiple features, these animals can stick strongly to smooth and rough surfaces alike but also can dart at a high speed while hanging onto a vertical surface. It has been shown that variety of physical mechanisms, apart from viscoelasticity, play important roles in enhancement and modulation of adhesion for these adhesive layers: crack initiation and arrest [10–12], surface friction [13,14], compressive surface stress [15] and self adhesion, and debonding [16]. While the role of the geometric features of the adhesive patterns is now fairly understood, the effect of spatial variation in the shear modulus of these layers has not been looked at in detail. In fact, it is highly unlikely that the effective modulus of these adhesives should remain same all through, for example, it should vary because of the surface and subsurface buried microstructures within these layers [17,18]. Therefore, the question remains as to how this spatial modulation should affect the fracture toughness, durability and susceptibility to environment of these adhesives. In this paper, we analyze this problem by considering a model adhesive which remains bonded to a rigid substrate while a flexible plate is lifted off it in a displacement controlled experiment [19]. The shear modulus of this adhesive is assumed to vary spatially. For simplicity, we consider that modulus varies only in one direction remaining independent along the others. Furthermore, we consider peeling of a flexible adherent in contact with the adhesive such that the crack propagates along the direction in which the modulus of the adhesive varies. We show that as against smooth and continuous peeling off an elastic layer with uniform modulus, here the crack propagates rather discontinuously with intermediate crack arrests and initiations. Crack gets arrested at the vicinity of the location of lowest modulus only to initiate again at a large enough applied torque. Once initiated, the crack propagates catastrophically till it is arrested again at the vicinity of the next location where the modulus reaches the minima. This process then results in increase in fracture toughness of the adhesive over the one with uniform modulus. In addition to thickness of the film, the fracture toughness is found also to be a function of the amplitude of variation in modulus and its wavelength.

II. PROBLEM FORMULATION

A. Experimental geometry

Fig. 1 depicts the schematic of an experiment in which a thin layer of an incompressible elastic adhesive having spatially varying modulus remains strongly bonded to a rigid substrate and a flexible plate is brought in partial contact with it so that a cusp shaped crack appears at the contact of the plate and the film. The initial distance of the point of application of the load from the contact line is adjusted by placing a spacer of desired height at the opening of the crack. The plate is then lifted in a displacement controlled manner

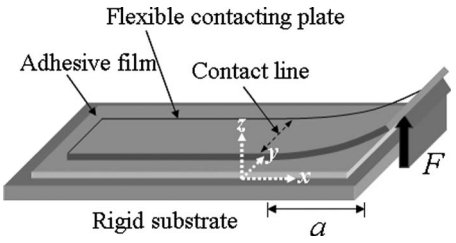

FIG. 1. Schematic of the experiment.

by applying a load on its hanging end. With progressive lifting of the plate, the lifting load increases while the contact line propagates away from the point of application of the load. Thus, we consider here one dimensional opening of a crack: its propagation along $-x$ direction remaining parallel to y. This description of the adhesive with spatially varying modulus is in fact inspired by two recent experiments: in one, the adhesive layer is patterned by incising it laterally along direction normal to propagation of the crack using a sharp razor blade [10,11]. The incisions span whole through the thickness of the layer or partially resulting in the elastic modulus of the adhesive dropping effectively to zero at the location of the incisions. Similarly, in another set of experiments, microchannels of appropriate diameter and cross-sections are embedded within the adhesive layer at desired vertical locations [15,16]. Several such channels are placed parallel to each other in a direction normal to the propagation of the crack, i.e., the contact line between the adhesive and the flexible adherent. The microchannels are either filled with air or a liquid of desired viscosity and surface tension resulting in continuous and periodic variation in the effective modulus of the adhesive. Variation in modulus of several functional forms can be generated by suitably choosing the channels and the fluid inside. Similar to the experiments considered here, in both these cases, the adhesive remains strongly bonded to a rigid substrate and a flexible adherent is lifted off it at a constant rate while the lifting load is measured. Nevertheless, despite similarities, these geometries do not exactly conform to the experiment considered here because of several complications; for example, in the case of the "microfluidic adhesive," along with the spatial variation in modulus, the surface of the layer too bulges out at the location of channels resulting in periodic undulations. Similarly, for the incision patterned adhesive, the surface does not remain continuous and the modulus varies discontinuously in steps. Here we choose to focus on the variation in modulus of the adhesive leaving aside its geometric variation, which has been investigated thoroughly in literature in different contexts.

B. Stress equilibrium relations

Simplicity of the above geometry allows us to assume plane strain approximation for analyzing the problem, i.e., displacement and stress field in the film remains independent along the y axis. Furthermore, assuming that the shear modulus of the film varies along x remaining independent of thickness of the layer, $\mu=\mu_0 \cdot f(x)$, we write the following stress equilibrium equation in terms of the hydrostatic pressure $p(x)$ within the film:

$$-\frac{\partial p}{\partial x}+\mu\left(\frac{\partial^2 u}{\partial x^2}+\frac{\partial^2 u}{\partial z^2}\right)+2\frac{\partial \mu}{\partial x}\frac{\partial u}{\partial x}=0$$

$$-\frac{\partial p}{\partial z}+\mu\left(\frac{\partial^2 w}{\partial x^2}+\frac{\partial^2 w}{\partial z^2}\right)+\frac{\partial \mu}{\partial x}\left(\frac{\partial u}{\partial z}+\frac{\partial w}{\partial x}\right)=0, \qquad (1)$$

where, u and w are the position dependent displacements in the film along x and z directions, respectively. The incompressibility of the film results in

$$\frac{\partial u}{\partial x}+\frac{\partial w}{\partial z}=0. \qquad (2)$$

These equations are solved using the following set of boundary conditions (b.c.).

(a) We use no slip boundary condition at the interface of the film and the substrate $(z=0)$, which implies $u(z=0)=w(z=0)=0$.

(b) At the interface of the film and the flexible plate, i.e., at $z=h$, we assume that the film adheres perfectly with the plate which undergoes small bending because of peeling. Hence, the lateral and the vertical displacements of the film at $z=h$ are expressed as: $u(z=h)=0$, $w(z=h)=\psi$, where ψ defines the vertical displacement of the plate; at $x<0$, it defines also the deformation of the film at $z=h$.

(c) Continuity of normal stress across the interface $(z=h)$ results in normal stress being equal to the bending stress on plate

$$\sigma_{zz}|_{z=h}=-D\frac{\partial^4 \psi}{\partial x^4} \quad \text{at } x<0, \qquad (3)$$

where, D is the flexural rigidity of the plate. At $0<x<a$, there is no traction either on the film or the plate, which yields

$$\sigma_{xz}|_{z=h}=\sigma_{zz}|_{z=h}=0. \qquad (4)$$

The boundary condition right at the contact line, i.e., at $x=0$ is, however, not obvious and requires some discussions. Classical theory of fracture mechanics for brittle material suggests that a singular stress field is maintained at the crack tip in order that the crack propagates. Soft deformable materials like elastomers, however, undergo deformation resulting in finite radius of the crack tip. In such a situation, the stress field cannot asymptotically reach to infinity but to a finite value which should remain maximum [20]. In essence, in order that the crack propagates on the surface of the film, the normal stress at the crack tip is always maintained at a critical level which results in the boundary condition: $\sigma_{zz}|_{x=0}=\sigma_c$. This critical stress is an intrinsic property of the elastomer and remains independent of the geometry of the experiment [21]. However, whether it should remain independent also of the material properties of the elastomer is debatable, because in the molecular level, formation and failure of the bonds at the interface is a statistical process which gets biased by the externally applied stress. As the debonding stress increases, more bonds fail than they appear; eventually, at a critical stress, all these bonds break catastrophically resulting in the macroscopic propagation of the crack [22]. It is then natural that the critical stress should depend upon the number of such interfacial bonds which in turn should depend upon the crosslinking density of the elastomer. However, in our calculation, the critical stress σ_c is kept constant by considering that the crosslinking density at the surface of the elastic layer remains unaltered while that at its bulk may vary. This situation, in a way, imitates the experiments on adhesive layers embedded with fluid filled microstructures, in which, leaving aside many other complexities, effectively the flexible adherent always remains in contact with a layer of constant crosslinking density while the local modulus of

the layer varies at the vicinity of the embedded structures. Thus, instead of modulus dependent critical stress at the crack tip we consider a constant critical stress. Based on our previous experiments on elastic layer with uniform modulus [10,19], here, we have carried out calculation for a range of critical stress values: $\sigma_c \sim 10^4 - 2\times 10^5$ N/m^2.

C. Dimension analysis

Equations (1) followed by the boundary conditions present a set of nonlinear partial differential equations, which are not amenable to analytical solutions. However, in order to have a better theoretical understanding, we can simplify these set of equations by considering only the dominant terms while eliminating the ones which are negligibly small. In this context, it is important to compare the characteristic lengths along x and z over which the displacements and stresses vary. In fact it is easy to show that the characteristic length L along x is considerably larger than that along z, e.g., the layer thickness h. It has been shown earlier in the context of peeling off a layer of constant modulus, i.e., $\mu=\mu_0$, that the normal stress on such a layer remains oscillatory with exponentially diminishing amplitude. The wavelength of such oscillation was deduced to be a function of the material and geometric properties of the adhesive and the adherent [19]: $L \sim 6q^{-1}=6(\frac{Dh^3}{12\mu})^{1/6}$, where D is the flexural rigidity of the plate and μ is the shear modulus of the layer [19,23]. It is natural to accept L as the characteristic length along x as it defines the length scale of spatial variation in stresses. The typical values of L can be obtained by substituting representative values for different parameters. For example, for $h=300$ μm, shear modulus $\mu=10^6$ N/m^2, and $D=0.02$ Nm, the characteristic length $L \sim 3.6$ mm, similarly, for $h=800$ μm, the same quantity is calculated as 5.84 mm; thus L is found to be considerably large than h over a large range of layer thickness. Using these characteristic quantities, we can then replace the differential operators in Eq. (1),

$$\frac{\partial}{\partial x} \sim \frac{1}{L}, \quad \frac{\partial^2}{\partial x^2} \sim \frac{1}{L^2}, \quad \frac{\partial}{\partial z} \sim \frac{1}{h}, \quad \text{and} \quad \frac{\partial^2}{\partial z^2} \sim \frac{1}{h^2}, \tag{5}$$

which allows us to identify terms, which are of orders $0(\frac{h^2}{L^2})$ and are thus negligibly small with respect to the others. This process results in the following equations:

$$\frac{\partial p}{\partial x} = \mu_0 f(x) \frac{\partial^2 u}{\partial z^2},$$

$$\frac{\partial p}{\partial z} = 0, \tag{6}$$

which appear similar to that derived for the earlier case [19] except that the constant modulus is replaced by a spatially varying modulus. Solution of Eq. (6) subjected to the boundary conditions yield the following relations for the displacements within the film, at $x<0$

$$u = \frac{1}{2\mu_0 f(x)} \frac{\partial p}{\partial x}(z^2 - zh),$$

$$w = \frac{1}{2\mu_0}\left(\frac{1}{f(x)}\frac{\partial^2 p}{\partial x^2} - \frac{1}{(f(x))^2}\frac{df(x)}{dx}\frac{dp}{dx}\right)\left(\frac{z^2 h}{2} - \frac{z^3}{3}\right). \tag{7}$$

The expressions in Eq. (7) incorporate the effect of functional variation in the modulus and its derivative, which influence the propagation of crack during peeling of the flexible plate. Here, we will demonstrate this effect by assuming that the modulus varies sinusoidally along the direction of propagation of the crack: $f(x)=1+\delta \sin kx$, where $k=2\pi/\lambda$ is the wave number and λ is the wavelength. Using this functional form in Eq. (7) and applying the boundary condition [(b) and (c)] at the surface of the film, we obtain the expression for displacement of the plate $\psi=w(z=h)$

$$\psi = \frac{Dh^3}{12\mu_0}\left\{\frac{1}{[1+\delta\sin(kx)]}\frac{\partial^6\psi}{\partial x^6} - \frac{\delta k\cos(kx)}{[1+\delta\sin(kx)]^2}\frac{\partial^5\psi}{\partial x^5}\right\}$$

at $x<0$,

$$\frac{\partial^4\psi}{\partial x^4} = 0 \quad \text{at } 0<x<a. \tag{8}$$

We solve Eqs. (8) with the boundary conditions that the displacement of the contacting plate, the shear force on it and the bending moment are continuous at $x=0$, which imply that displacement ψ and its first to third order derivatives are continuous at the contact line. In addition, the displacements of plate satisfy two more boundary conditions: at $x=a$ the plate remains freely supported, which yields $\psi|_{x=a}=\Delta$, $\psi_{xx}|_{x=a}=0$. Furthermore, far away from the contact line, at $x\to-\infty$ the vertical displacement of the plate vanishes asymptotically implying that the displacement ψ and its first and third order derivatives vanish at $x\to-\infty$.

Equations (8) present a set of differential equations in which nonlinearity occurs because of the spatial variation in modulus. These equations subjected to boundary conditions are solved numerically for different values of σ_c, film thickness h, wave number k, and amplitude δ of the shear modulus. In the next section, we discuss in detail the results of these calculations.

III. RESULTS AND DISCUSSIONS

A. Lift off force

Figure 2 shows the lift force to be applied on the hanging end of the plate in order to drive an interfacial crack. While for a layer with uniform modulus, the load decreases continuously with increase in the distance a of the contact line from the point of application of the load, for a film with periodic variation in modulus, the load too varies in a periodic manner but discontinuously, showing stick slip behavior. Curves 1, 2′, and 3′ representing layers of modulus $\mu=10^6$, 10^5, and 2×10^4 N/m^2 show the force vs displacement of the former kind; whereas curves 2–4 for $\mu_0=10^6$ N/m^2 and $\delta=0.5$, 0.9, and 0.98, respectively, bring out the crack arresting effect. For example, in curve 3, point A signifies the location, at which the modulus of the layer is at its mean value, $\mu=\mu_0=10^6$ N/m^2, so that the applied load F coincides with that is calculated for curve 1. However,

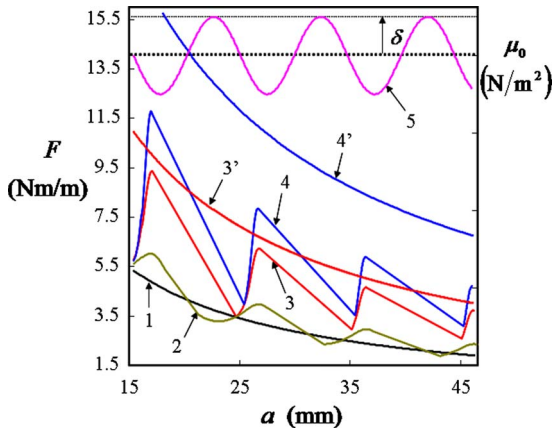

FIG. 2. (Color online) Typical plots of peel off force as a function of position of the contact line from the point of application of the load for various amplitudes of variation in modulus. The data represents peeling off an elastic film of thickness $h=500$ μm under crack tip critical stress $\sigma_c=7.5\times10^4$ N/m^2. Curves 1, 3′, and 5′ represent elastic layers of uniform modulus: $\mu=10^6$, 10^5, and 2×10^4 N/m^2, respectively. Curves 2–4 represent elastic layers of modulus, $\mu=10^6[1+\delta\sin(0.65x)]$ N/m^2 (x is in mm) and $\delta=0.5$, 0.9, and 0.98, respectively. Curve 5 depicts the sinusoidal variation in modulus along the direction of propagation of crack front.

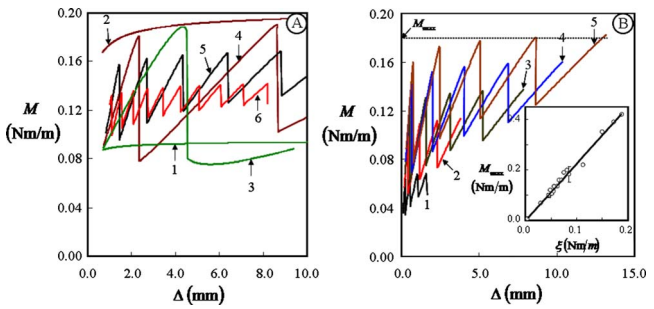

FIG. 3. (Color online) The torque M for lifting the flexible plate plotted against the displacement Δ at its hanging end show the crack arrest and catastrophic initiation phenomena. (A) Curves 1 and 2 are plotted for elastic layers of thickness $h=800$ μm and uniform modulus $\mu=10^6$ and 10^5 N/m^2, respectively. Curves 3–6 represent films with spatially varying modulus $\mu=10^6[1+0.9\sin(kx)]$ N/m^2 with wave number $k=0.1$, 0.26, 0.77, and 1.03 mm^{-1}, respectively. (B) Curves 1–5 represent layers of modulus $\mu=10^6[1+0.9\sin(0.5x)]$ N/m^2 and thickness $h=300$, 500, 600, 700, and 800 μm, respectively. The inset shows that the maximum torque $M_{\max}$ data from variety of experiments scale linearly with the quantity $\xi=(1-\delta)^{-1/5}(\sigma_c h)(D/12\mu_0)^{1/3}$ with slope 2.255.

beyond this point, in the range A and B, the modulus decreases with concomitant increase in the lifting load, while the crack remains almost arrested. The load reaches maxima at point B, which is rather close to the location of minimum shear modulus of the layer. Beyond this point, the modulus increases so that the equilibrium load required to drive the crack is smaller than F at B. As a result, the crack propagates rather catastrophically to the region of increasingly higher modulus, eventually crossing the point C of maximum modulus. Finally, it slows down and almost stops at the vicinity of the minimum modulus of the layer at D. This cycle of crack arrest and catastrophic propagation is similar to that observed with incision patterned elastic films [10,11] and films with embedded microstructures [15,16]. It is appropriate to mention here that even during catastrophic propagation, maximum crack speed is rather small [15] ~0.3 mm/s, which allows the equilibrium of forces at the interface of the adherents. Nevertheless, these observations imply that the local variation in deformability or the compliance of the adhesive layer engendered by the patterns on its surface or at its bulk and even uniformly thin layers but with spatially varying modulus lead to stick slip crack propagation. Curves 2–4 in Fig. 2 show also that this effect gets more prominent for layers for which modulus varies with larger amplitude. When the amplitude is small, e.g., for $\delta=0.5$ (curve 2), the lift off force varies periodically about that for the mean modulus (curve 1), however for large enough amplitude (curves 3 and 4), the lift off force is calculated to be always higher than that for the mean modulus.

B. Lifting torque

The effect of enhanced deformability of the layers is further investigated by calculating the effective torque applied at the hanging end of the flexible plate. Figure 3 shows the plot of lift off torque $M=F\cdot a$ with respect to the vertical displacement Δ of the hanging end of the plate. As against continuously varying torque calculated for layers with uniform modulus, here torque varies discontinuously signifying crack arrest and initiation. M increases with increase in Δ as the contact line remains stationary at the vicinity of the microchannel, however decreases catastrophically as the crack initiates at a critical torque. The lift off torque is calculated for layers of variety of thickness, $h=300-800$ μm, critical stress, $\sigma_c=1\times10^4-2\times10^5$ N/m^2, amplitude $\delta=0-0.95$, and wave number $k=0.1-1.5$ mm^{-1} of periodic variation in the modulus of the layer. These values of the parameters are similar to those in which experiments were conducted on smooth adhesive films and the ones with surface and subsurface patterns. For example, in experiments in which flexible glass plates are peeled off smooth and patterned elastomeric layers of poly(dimethylsiloxane) (PDMS), the critical crack opening stress is estimated as [19] $\sim4\times10^4-2\times10^5$ N/m^2. Similarly, in experiments with microchannel embedded adhesives [15], the lateral space λ between the channels is maintained at 3–10 mm. Calculations with above range of parameter values yield a maximum torque $M_{\max}$, which increases slightly as the contact line moves further away from the point of application of the load, an observation seen also during peeling off a microchannel embedded adhesive film [15]. The curves 1 and 2 in Fig. 3(a) calculated for $\mu=10^6$ and 10^5 N/m^2, respectively, show that for layers with uniform modulus, the torque required to propagate the crack increases significantly with decrease in μ. This has to do with the increase in compliance of the layer which increases with the quantity [24,25] h^3/μ. In the context of elastic layers with spatially varying modulus, the compliance is also a function of the length scale of this variation. For example, curves 3–6 in Fig. 3(a) computed for layers with

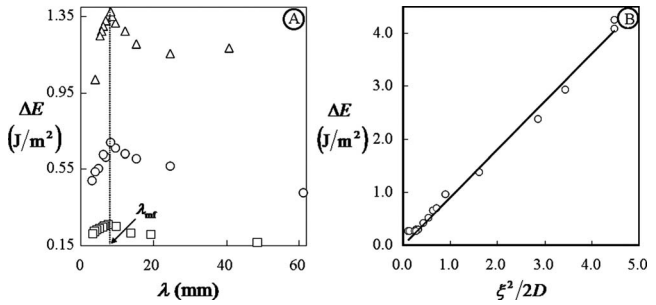

FIG. 4. (A) Fracture toughness ΔE of the interface plotted against the wavelength of modulus variation λ show that ΔE maximizes for an intermediate wavelength. The symbols △ and ○ represent data computed for a film of thickness $h=800$ μm and shear modulus $\mu=10^6[1+0.9\sin(kx)]$, $k=2\pi/\lambda$ using critical stress $\sigma_c=5\times10^4$ and 7.5×10^4 N/m^2, respectively. Symbol □ represents $h=500$ μm $\mu=10^6[1+0.9\sin(kx)]$ and $\sigma_c=5\times10^4$ N/m^2. (B) The fracture toughness data from different experiments are plotted against $\zeta=\xi^2/2D$ with the result $\Delta E=0.905(2.255)^2(1-\delta)^{-2/5}(\sigma_c h)^2(D/12\mu_0)^{2/3}/2D$.

$\mu_0=10^6$ N/m^2, $\delta=0.9$, and $k=0.1$, 0.26, 0.77, and 1.03 mm^{-1}, respectively, depict the effect of wavelength of variation in modulus on the maximum crack initiation torque, $M_{\max}$. When the wavelength is large, the layer gets maximally compliant so that at the location of minimum modulus, the maximum torque $M_{\max}$ coincides with that computed for $\mu=10^5$ N/m^2. However, as the wavelength decreases, the nonlinear coupling of the gradients of modulus and the stress fields result in decrease in $M_{\max}$ which eventually approaches a value intermediate to curves 1 and 2. The maximum torque $M_{\max}$ however increases significantly with the increase in h, σ_c, and δ. The M vs Δ data in Fig. 3(b) plotted for $h=300-800$ μm depict the dependence of maximum torque $M_{\max}$ on thickness of the layers. In fact, calculation with different values of these parameters show that $M_{\max}$ scales linearly with the quantity $\xi=(1-\delta)^{-1/5}(\sigma_c h)(D/12\mu_0)^{1/3}$ (Fig. 3) with slope 2.255, which corroborates well with similar relation for $M_{\max}$ derived for incision patterned adhesives [10,11]. The error bars in this figure are obtained for calculations with different values of the wave number $k=0.65\pm0.15$ mm^{-1}. Here, the torque data for intermediate values of wave number, i.e., $k=0.65\pm0.15$ mm^{-1} are considered, because the fracture toughness of the interface, estimated as the area under the force vs displacement plot, is found to maximize within this range of values of the wave number as shown in Fig. 4(a). These results are consistent with the observations in experiments with "microfluidic adhesives" where the fracture toughness maximizes at an intermediate separation between the embedded channels. For small wave number, the regions of minimum modulus of the layer remain further apart; as a result, an interfacial crack propagates continuously for longer period than while remaining arrested at the close vicinity of the location of the minimum modulus. With increase in wave number, i.e., decrease in wavelength, the crack gets arrested more often, as a result, the fracture toughness of the interface increases. However, decrease in the wavelength of modulus variation is also accompanied by the decrease in the crack initiation force which leads to decrease in the area under the force vs. displacement curve. Thus, two opposing effects of wavelength result in an optimum intermediate range of wavelength at which the fracture energy attains a maxima.

C. Fracture toughness

Beside wavelength, fracture energy of the interface depends also on the thickness of the layers h and the critical stress σ_c at the crack tip. This behavior is similar to the maximum crack initiation torque. In Fig. 4(a), the ΔE data plotted for $h=500-800$ μm and $\sigma_c=5\times10^4$ and 7.5×10^4 N/m^2 depict this effect: ΔE increases with both h and σ_c. This dependence can be rationalized by using our earlier results for continuous peeling of a flexible adherent off a smooth layer of adhesive [19] for which the toughness increases with the lifting torque on plate as, $\Delta E\sim M^2/2D$. Since, in our experiments, maximum torque scales linearly with the quantity, $M_{\max}=2.255\xi$, it is expected that the fracture toughness should vary linearly with the quantity $\xi^2/2D$. Indeed Fig. 4(b) shows that ΔE vary linearly with the quantity $\zeta=(2.255)^2(1-\delta)^{-2/5}(\sigma_c h)^2(D/12\mu_0)^{2/3}/2D$ with slope 0.905 which is very close to the theoretical value of 1.0. Thus, we obtain a scaling relation for fracture toughness ΔE of the interface with various material and geometric properties of the adherents. Furthermore, the calculated values of ΔE are similar to those observed in experiments with adhesives embedded with subsurface structures. For example, for $h=800$ μm, the ΔE value is calculated as 1.2–1.4 J/m^2, which corroborates well with that obtained from experiments with microchannel embedded adhesives ~1.8 J/m^2. Although the above calculations corroborate with many observations in experiments with patterned adhesives, it does not replicate the adhesion mechanism completely. For example, for the michrofluidic adhesive, adhesion strength is influenced also by the Laplace pressure of the liquid inside the channels besides being affected by the variation in the effective modulus of the layers as considered here.

IV. SUMMARY

We have presented here a theoretical analysis of peeling a flexible plate off a layer of elastic adhesive, the shear modulus of which oscillates about a mean value along the direction of peeling. Calculations show that an interfacial crack on such an adhesive does not propagate continuously, but intermittently with crack arrests close to the locations of minimum modulus of the layers and subsequent crack initiations at a critical lifting torque. Once initiated, the crack propagates catastrophically till it is arrested again at the vicinity of the subsequent minimum modulus. As a result, the

adhesion toughness of such an adhesive layer is calculated to be higher than that for a layer with the mean uniform modulus. These results corroborate with the recent experimental observations for elastic layers with embedded microstructures for which fluid filled microchannels buried underneath the adhesive enhance interfacial adhesion significantly. We have calculated also the effect of critical stress at the crack tip and the amplitude of variation in modulus of the elastic layer and obtained the scaling laws which can help in defining the optimal values of geometric and physical characteristics of such adhesives.

ACKNOWLEDGMENTS

A.G. acknowledges Professor Manoj K. Chaudhury for suggesting this problem. A.G. acknowledges also an IRHPA grant from Department of Science and Technology, Government of India for this work.

[1] K. Autumn, Y. A. Liang, S. T. Hsieh, W. Zesch, W. P. Chan, T. W. Kenny, R. Fearing, and R. J. Full, Nature (London) **405**, 681 (2000).
[2] M. Scherge and S. N. Gorb, *Biological Micro- and Nanotribology: Nature' Solutions* (Springer, New York, 2001).
[3] R. Spolenak, S. N. Gorb, H. Gao, and E. Arzt, Proc. R. Soc. London, Ser. A **461**, 305 (2005).
[4] S. N. Gorb, Y. Jiao, and M. J. Scherge, J. Comp. Physiol. [A] **186**, 821 (2000).
[5] S. N. Gorb, S. Niederegger, C. Y. Hayashi, A. P. Summers, W. Vötsch, and P. Walther, Nature (London) **443**, 407 (2006).
[6] C. Creton and S. N. Gorb, MRS Bull. **32**, 466 (2007).
[7] J. D. Gillett and V. B. Wigglesworth, Proc. R. Soc., London, Ser. B **111**, 364 (1932).
[8] J. M. Smith, W. J. P. Barnes, J. R. Downie, and G. D. Ruxton, J. Comp. Physiol. [A] **192**, 1193 (2006).
[9] W. Federle, W. J. P. Barnes, W. Baumgartner, P. Drechsler, and J. M. Smith, J. R. Soc., Interface **3**, 689 (2006).
[10] A. Ghatak, L. Mahadevan, J. Y. Chung, M. K. Chaudhury, and V. Shenoy, Proc. R. Soc. London, Ser. A **460**, 2725 (2004).
[11] J. Y. Chung and M. K. Chaudhury, J. R. Soc., Interface **2**, 55 (2005).
[12] N. J. Glassmaker, A. Jagota, C.-Y. Hui, W. L. Noderer, and M. K. Chaudhury, Proc. Natl. Acad. Sci. U.S.A. **104**, 10786 (2007).
[13] Y. Tian, N. Pesika, H. Zeng, K. Rosenberg, B. Zhao, P. McGuiggan, K. Autumn, and J. Israelachvili, Proc. Natl. Acad. Sci. U.S.A. **103**, 19320 (2006).
[14] L. Ge, S. Sethi, L. Ci, P. M. Ajayan, and A. Dhinojwala, Proc. Natl. Acad. Sci. U.S.A. **104**, 10792 (2007).
[15] A. Majumder, A. Ghatak, and A. Sharma, Science **318**, 258 (2007).
[16] E. P. Arul and A. Ghatak, Langmuir **25**, 611 (2009).
[17] S. T. Chang, A. B. Uçar, G. R. Swindlehurst, O. Robert, O. Bradley IV, F. J. Renk, D. Orlin, and O. D. Velev, Adv. Mater. **21**, 2803 (2009).
[18] A. Majumder, A. K. Tiwari, K. Korada, and A. Ghatak, J. Adhes. Sci. Technol. (to be published).
[19] A. Ghatak, L. Mahadevan, and M. K. Chaudhury, Langmuir **21**, 1277 (2005).
[20] C.-Y. Hui, J. M. Baney, and E. J. Kramer, Langmuir **14**, 6570 (1998).
[21] D. S. Dugdale, J. Mech. Phys. Solids **8**, 100 (1960).
[22] A. Ghatak, K. Vorvolakos, H. She, D. L. Malotky, and M. K. Chaudhury, J. Phys. Chem. B **104**, 4018 (2000).
[23] D. A. Dillard, ASME J. Appl. Mech. **56**, 382 (1989).
[24] W. L. Noderer, L. Shen, S. Vajpayee, N. J. Glassmaker, A. Jagota, and C.-Y. Hui, Proc. R. Soc. London, Ser. A **463**, 2631 (2007).
[25] F. Yang, J. Phys. D **35**, 2614 (2002).